

# Template Synthesis of Hollow Sb Nanoparticles as a High-Performance Lithium Battery Anode Material

Hyesun Kim and Jaephil Cho\*

Department of Applied Chemistry, Hanyang University,  
Ansan, Korea 426-791

Received November 29, 2007

Revised Manuscript Received January 29, 2008

Lithium reactive Sb-based alloys have been investigated as a possible candidate among metallic anode materials for replacing the graphite currently used as a lithium battery anode material.<sup>1–9</sup> These materials have been showed large degree of volume expansion and contraction during lithium alloy and dealloy processes, resulting in a rapid capacity fade. Given that lithium–metal alloys have an ionic character, it is, therefore, very easy to pulverize during lithium alloying and dealloying.<sup>10</sup> This pulverization results in an electrical disconnect between the particles and current collectors, resulting in rapid capacity fading. To improve the capacity retention of lithium reactive metal alloys, many attempts, such as the formation of mesopores,<sup>11–14</sup> the use of metal and carbon composites,<sup>15–20</sup> and the introduction of nano-sized metals,<sup>21–25</sup> have been reported. Studies involving hollow lithium reactive metal, however, have yet to be

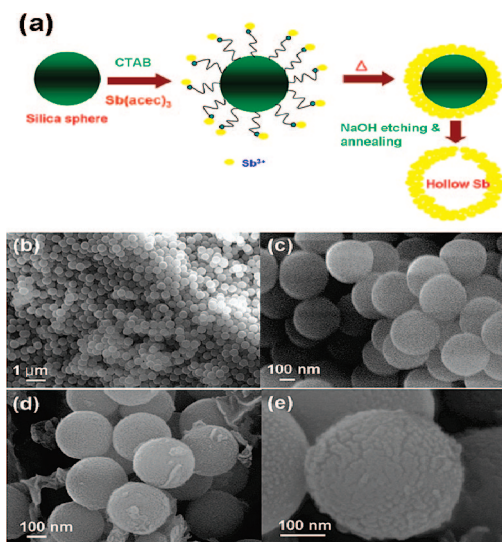


**Figure 1.** (a) Schematic diagram of the preparation of hollow Sb particles from the CTAB-functionalized  $\text{SiO}_2$  template. (b, c) SEM images of the  $\text{SiO}_2$  template, and (d, e) SEM images of the  $\text{SiO}_2$  template coated with Sb particles.

reported, although investigations of hollow  $\text{SnO}_2$ <sup>26–28</sup> have been carried out. The use of hollow  $\text{SnO}_2$  led to improved specific capacity and capacity retention characteristics compared to  $\text{SnO}_2$  nanoparticles.

On the other hand, hollow spheres of various materials, including oxides, metals, and semiconductors, have been created via template approaches for possible new opportunities in catalysis, microelectronics, and photonics.<sup>29–31</sup> Among the various types of hollow materials, hollow metals using silica and polymers as well as those without templates have been studied.<sup>32–40</sup> For instance, Kim et al. reported that hollow Pd spheres was obtained after coating functionalized

\* Corresponding author. E-mail: jpcho@hanyang.ac.kr.

- (1) Li, H.; Shi, L.; Lu, W.; Huang, X.; Chen, L. *J. Electrochem. Soc.* **2001**, *148*, A915.
- (2) Yang, J.; Takeda, Y.; Imanishi, N.; Yamamoto, O. *J. Electrochem. Soc.* **1999**, *146*, 4009.
- (3) Fransson, L. M. L.; Vaughey, J. T.; Benedek, R.; Edstrom, K.; Thomas, J. O.; Thackeray, M. M. *Electrochem. Commun.* **2001**, *3*, 317.
- (4) Ren, J.; He, X.; Pu, W.; Jiang, C.; Wan, C. *Electrochim. Acta* **2006**, *52*, 1538.
- (5) Pralong, V.; Leriche, J. B.; Beaudoin, B.; Naudin, E.; Morctette, M.; Tarascon, J. M. *Solid State Ionics* **2004**, *166*, 295.
- (6) Fernandez Madrigal, F. J.; Lavela, P.; Perez-Vicente, C.; Tirado, J. L. *J. Electroanal. Chem.* **2001**, *501*, 205.
- (7) Fransson, L. M. L.; Vaughey, J. T.; Edstrom, K.; Thackeray, M. M. *J. Electrochem. Soc.* **2003**, *150*, A86.
- (8) Zhao, X. B.; Cao, G. S. *Electrochim. Acta* **2001**, *46*, 891.
- (9) Hewitt, K. C.; Beaulieu, L. Y.; Dahn, J. R. *J. Electrochem. Soc.* **2001**, *148*, A402.
- (10) Wachtler, M.; Besenhard, J. O.; Winter, M. *J. Power Sources* **2001**, *94*, 189.
- (11) Kim, E.; Son, D.; Kim, T.-G.; Cho, J.; Park, B.; Ryu, K. S.; Chang, S. H. *Angew. Chem., Int. Ed.* **2004**, *43*, 5987.
- (12) Kim, E.; Kim, M. G.; Kim, Y.; Cho, J. *Electrochem. Solid-State Lett.* **2005**, *8*, A452.
- (13) Kim, H.; Park, G.-S.; Kim, E.; Kim, J.; Doo, S. -G.; Cho, J. *J. Electrochem. Soc.* **2006**, *153*, A1633.
- (14) Kim, J.; Cho, J. *Electrochem. Solid-State Lett.* **2006**, *9*, A373.
- (15) Kim, E.; Kim, M. G.; Cho, J. *Electrochem. Solid-State Lett.* **2006**, *9*, A311.
- (16) Li, H.; Wang, Q.; Shi, L.; Chen, L.; Huang, X. *Chem. Mater.* **2002**, *14*, 103.
- (17) Wang, Y.; Lee, J. Y.; Deivaraj, T. C. *J. Electrochem. Soc.* **2004**, *151*, A1804.
- (18) Kim, I.-S.; Blomgren, G. E.; Kumta, P. N. *Electrochem. Solid State Lett.* **2004**, *7*, A44.
- (19) Lee, K. T.; Jung, Y. S.; Oh, S. M. *J. Am. Chem. Soc.* **2003**, *125*, 5652.
- (20) Noh, M.; Kwon, Y.; Lee, H.; Cho, J.; Kim, Y.; Kim, M. G. *Chem. Mater.* **2005**, *17*, 1926.
- (21) Wang, Y.; Lee, J. Y.; Deivaraj, T. C. *J. Mater. Chem.* **2004**, *14*, 362.
- (22) Yin, J.; Wada, M.; Yoshida, S.; Ishihara, K.; Tanse, S.; Sakai, T. *J. Electrochem. Soc.* **2003**, *150*, A1129.

- (23) Yin, J.; Wada, M.; Tanase, S.; Sakai, T. *J. Electrochem. Soc.* **2004**, *151*, A583.
- (24) Lee, H.; Kim, H.; Doo, S.-G.; Cho, J. *J. Electrochem. Soc.* **2007**, *154*, A343.
- (25) Hwang, H.; Kim, M. G.; Cho, J. *J. Phys. Chem. C* **2007**, *111*, 1186.
- (26) Han, S.; Jang, B.; Kim, T.; Oh, S. M.; Hyeon, T. *Adv. Funct. Mater.* **2005**, *15*, 1845.
- (27) Lou, W.; Wang, Y.; Yuan, C.; Lee, J. Y.; Archer, L. A. *Adv. Mater.* **2006**, *18*, 2325.
- (28) Wang, Y.; Su, F.; Lee, J. Y.; Zhao, X. S. *Chem. Mater.* **2006**, *18*, 1347.
- (29) Caruso, F. *Adv. Mater.* **2001**, *13*, 11.
- (30) Breen, M. L.; Dinsmore, A. D.; Pink, R. H.; Qadri, S. B.; Ratna, B. R. *Langmuir* **2001**, *17*, 903.
- (31) Tierno, P.; Goedel, W. A. *J. Phys. Chem. B* **2006**, *110*, 3043.
- (32) Kim, S.-W.; Kim, M.; Lee, W. Y.; Hyeon, T. *J. Am. Chem. Soc.* **2002**, *124*, 7642.
- (33) Li, Q.; Liu, H.; Han, M.; Zhu, J.; Liang, Y.; Xu, Z.; Song, Y. *Adv. Mater.* **2005**, *17*, 1995.
- (34) Hu, Y.; Chen, J.; Chen, W.; Lin, X.; Li, X. *Adv. Mater.* **2003**, *15*, 726.
- (35) Chiang, R.-K.; Chiang, R.-T. *Inorg. Chem.* **2007**, *46*, 369.
- (36) Cao, X.; Gu, L.; Zhuge, L.; Gao, W.; Wang, W.; Wu, S. *Adv. Funct. Mater.* **2006**, *16*, 896.
- (37) Dhas, N. A.; Suslick, K. S. *J. Am. Chem. Soc.* **2002**, *124*, 7642.
- (38) von Werne, T.; Patten, T. E. *J. Am. Chem. Soc.* **1999**, *121*, 7409.
- (39) MacLachlan, M. J.; Manners, I.; Ozin, G. A. *Adv. Mater.* **2000**, *12*, 675.
- (40) Vasquez, Y.; Sra, A. K.; Schaak, R. E. *J. Am. Chem. Soc.* **2005**, *127*, 12504.

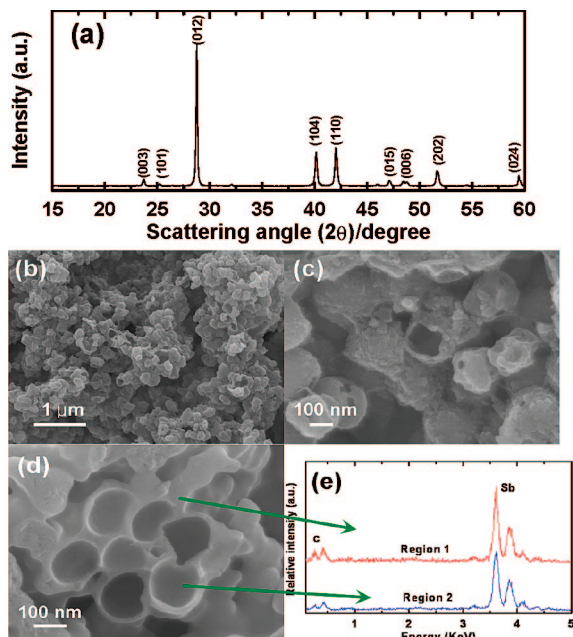


**Figure 2.** (a) XRD patterns of the as-prepared hollow Sb particles after thermal annealing at 400 °C, (b, c) SEM images of the as-prepared hollow Sb particles, and (d) SEM image of the cross-sectioned sample shown in (c). (e) EDX spectra of regions 1 and 2 in the SEM image shown in (d).

SiO<sub>2</sub> spheres with mercaptopropylsilyl groups followed by successive decomposition of Pd(acac)<sub>2</sub> in toluene at 250 °C.<sup>32</sup> Dhas et al. reported that hollow MoS<sub>2</sub>-coated SiO<sub>2</sub> nanoparticles were prepared with the thermal decomposition of Mo(CO)<sub>6</sub> in isodurene under an Ar flow, and the SiO<sub>2</sub> template was removed by etching in HF.<sup>40</sup>

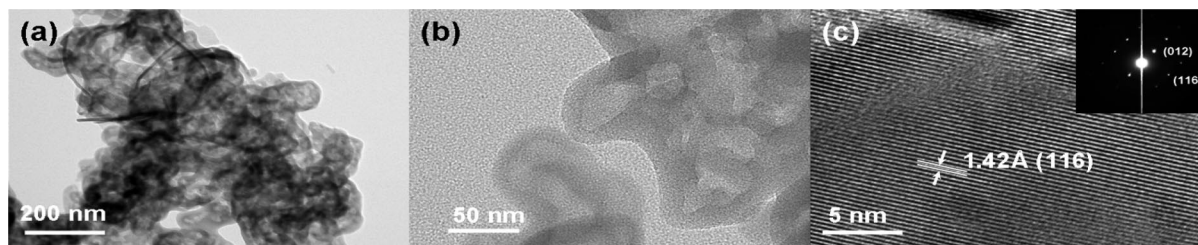
In the present study, the synthesis of hollow Sb particles using a SiO<sub>2</sub> template functionalized with cetyltrimethylammonium bromide (CTAB) groups is reported. Its electrochemical result shows superior cycling performance to nanosized Sb.

Figure 1a shows a schematic diagram of the preparation procedure of hollow Sb particles, and the initially prepared uniform silica template is shown. When the surfaces of the hollow Sb particles were functionalized with CTAB groups in ethanol, dissolved Sb precursor Sb(acac)<sub>3</sub> was then absorbed on the CTAB-functionalized template. The resulting template was heat-treated at 300 °C in an Ar atmosphere. SEM images of as-prepared SiO<sub>2</sub> template (b and c) and of Sb-coated template (d and e) were taken, and the SiO<sub>2</sub> templates are spherical with diameters of approximately 300 nm. After Sb coating, the original morphology remains. This was followed by NaOH etching and annealing at 400 °C for 1 h under a vacuum to remove the CTAB.

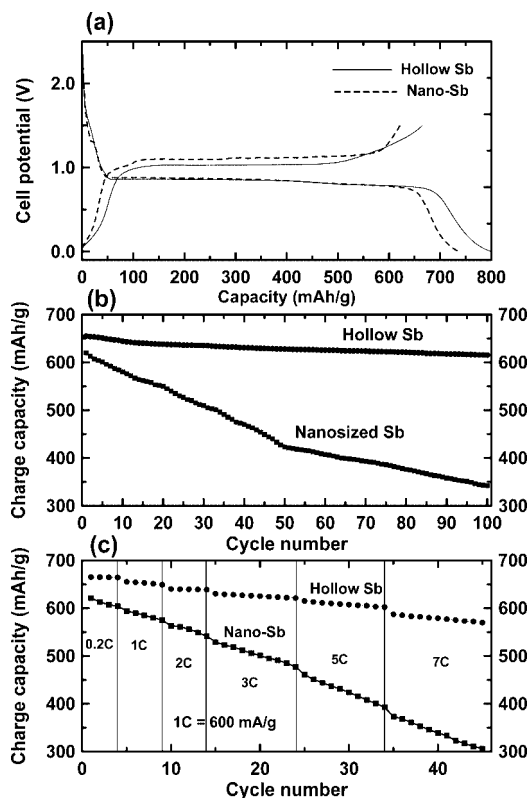
Figure 2a shows XRD patterns of the hollow Sb powder after NaOH etching and annealing at 400 °C under a vacuum. No secondary phases are observable. The diffraction patterns can be indexed to a rhombohedral structure with the  $R\bar{3}m$  space group, and the lattice constants were estimated as  $a = 4.306$  Å and  $c = 11.271$  Å. Images b and c in Figure 2 show SEM images of the hollow Sb. The empty cores in the Sb particles are clearly shown. Figure 2c shows a cross-sectioned SEM image of the hollow Sn particles with shell thicknesses of approximately 20 nm. The energy-dispersive X-ray spectra in the hollow sphere and shell regions confirm the pure Sb with no traces of Si detected at 1.7 KeV. Figure 3 shows TEM images of the hollow Sb particles with an empty core. The uniform shell thickness of nearly 20 nm agrees with that shown in the SEM results. A HREM image of shell (c) shows that the lattice fringes of the (116) plane correspond to 1.42 Å of Sb. The selected area diffraction pattern clearly shows the formation of single-crystalline Sb.

Figure 4a shows the voltage profiles of the hollow and nanosized Sb metals (SEM images of the nanosized Sb showing particle sizes of approximately 100 nm (see the Supporting Information, Figure S1)) during the first cycle. The discharge and charge capacities of the hollow Sb are 798 and 665 mAh/g, respectively, showing Coulombic efficiency of 83%, whereas those of the nanosized Sb are 732 and 620 mAh/g, respectively, showing a Coulombic efficiency of 84%. It is believed that the improved specific lithium storage capacity of the hollow Sb is largely associated with the unique structure of the hollow nanostructure, which has high porous shells that formed during NaOH etching. Figure 4b shows the cycle number vs the charge capacities of the hollow and nanosized Sb particles out to 100 cycles. The capacities of the hollow and nanosized Sb after 100 cycles are 615 and 342 mAh/g and have capacity retention ratios of 94 and 55%, respectively (note that hollow Sb was cycled at a rate of 1C). It is evident that the cycling performance of the hollow Sb is substantially improved while the nanosized Sb shows a large amount of capacity fade after 100 cycles.

Figure 4C exhibits the rate capabilities of the samples with increasing current rates from 0.2C to 7C (= 4200 mA/g), and hollow Sb shows superior charge capacity retention at higher rates to the nanoparticle counterpart. The hollow sample shows the first charge capacity and its capacity after 10 cycles at a 7C rate is 587 and 570 mAh/g, respectively.



**Figure 3.** (a) TEM images of the hollow Sb particles, and (b) an expanded image of (a). (c) Expanded image of the shell in (b) with the inset indicating the selected area diffraction pattern of (b).



**Figure 4.** (a) Voltage profiles of hollow and nanosized Sb particles between 0 and 1.2 V at a rate of 0.2 (=120 mA/g) in coin-type half-cells and (b) the corresponding charge capacities vs the cycle number (1C and 0.2C rates were used for the hollow and nanosized Sb particles, respectively). (c) Plot of charge capacity vs cycle number of hollow and nanosized Sb particles between 0 and 1.2 V at different current rates from 0.2C to 7C (discharge current rate was fixed at 0.2 C).

However, Sb nanoparticles shows 373 and 306 mAh/g at the same test conditions.

In contrast to the metal hosts (M), lithium alloys  $\text{Li}_x\text{M}$  are of highly ionic character and therefore they are usually fairly brittle. Thus, mechanical stresses, related with the volume changes, induce a rapid decay in mechanical stability. This is particularly true for coarse-grained, macrostructured

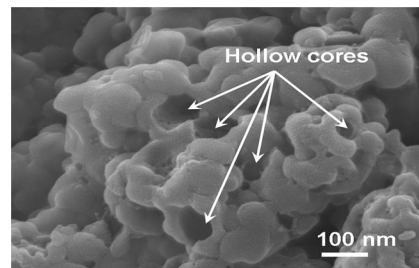


**Figure 5.** SEM image of the cycled hollow Sb electrode (after 100 cycles).

metals. However, mechanical strain has been reported to be reduced by tailoring the particle morphologies, such as particle size, shape, texture, and porosity, etc.<sup>1,4,11,26,27</sup> In our case, SEM image of the cycled hollow Sb particles clearly shows the presence of the hollow cores (Figure 5), indicating that the empty core can act as a buffer layer to accommodate the volume expansion of the shell.

In conclusion, Hollow Sb particles prepared from a CTAB-functionalized  $\text{SiO}_2$  template showed significantly improved capacity retention compared with previously reported Sb-related materials. This improvement was largely associated with the presence of hollow cores that acted as buffer layers for the volume change of the Sb shell. Because of the formation of the empty core, the volumetric energy density of the cell is expected to be decreased, compared to its solid counterpart. However, hollow metallic Sb anode demonstrated higher energy density than its solid counterpart at higher current rates.

**Acknowledgment.** This work was supported by the Korea Research Foundation Grant funded by the Korean Government (MOEHRD, Basic Research Promotion Fund) (KRF-2006-331-C00162).

**Supporting Information Available:** Experimental section and a SEM image of the Sb nanoparticles (PDF). This information is available free of charge via the Internet at <http://pubs.acs.org>.

CM703401U